

This is a non-peer reviewed preprint submitted to EarthArXiv. Subsequent peer-reviewed versions of this manuscript may have slightly different content. The authors welcome feedback.

Corresponding email address: sandy.herho@email.ucr.edu

1 Numerical simulation of the 2D trajectory of a
2 non-buoyant fluid parcel under the influence of
3 inertial oscillation

4 Sandy H. S. Herho^{1*}, Iwan P. Anwar², Katarina E. P. Herho³,
5 Candrasa S. Dharma⁴, Dasapta E. Irawan⁵

6 ^{1*}Department of Earth and Planetary Sciences, University of California,
7 900 University Ave., Riverside, 92521, CA, USA.

8 ²Oceanography Research Group, Bandung Institute of Technology
9 (ITB), Jalan Ganesha 10, Bandung, 40132, West Java, Indonesia.

10 ³Department of Geological Engineering, Trisakti University, Jalan
11 Letjen S. Parman 1, West Jakarta, 1440, DKI Jakarta, Indonesia.

12 ⁴Naval Hydrographic and Oceanographic Center (Pushidrosal),
13 Indonesian Navy (TNI AL), Jalan Pantai Kuta V/1, North Jakarta,
14 14310, DKI Jakarta, Indonesia.

15 ⁵Applied Geology Research Group, Bandung Institute of Technology
16 (ITB), Jalan Ganesha 10, Bandung, 40132, West Java, Indonesia.

17 *Corresponding author(s). E-mail(s): sandy.herho@email.ucr.edu;

18 **Abstract**

19 The trajectory of non-buoyant fluid parcels under the influence of inertial oscillations is a pivotal phenomenon in geophysical fluid dynamics, impacting processes such as tracer transport, pollutant dispersion, and the dynamics of marine organisms. This study presents a comprehensive numerical investigation of the two-dimensional trajectory of a non-buoyant fluid parcel subjected to inertial oscillations, complemented by abrupt external forcing events.

25 The simulations were implemented using multiple open-source, code-based general programming languages, including Fortran, Python, GNU Octave, R, and Julia. By running 1,000 iterations in each environment, we rigorously evaluated the computational performance and accuracy of these languages in tackling this idealized problem. The results, visualized through static plots and an animation generated using the Matplotlib library, capture the oscillatory trajectories

31 and the influence of rotational effects, validating the numerical models' ability to
32 represent the fundamental physics governing fluid motion.
33 Furthermore, a robust statistical analysis compared the execution times across the
34 programming environments. The Kruskal-Wallis test and Dunn's post-hoc test
35 with Bonferroni correction reveal that Fortran exhibits significantly faster exe-
36 cution times compared to the other environments, highlighting its suitability for
37 computationally intensive simulations in geophysical fluid dynamics. This study
38 provides valuable insights into selecting appropriate computational tools and con-
39 tributes to educational resources for teaching idealized fluid dynamics models,
40 laying the foundation for more sophisticated hierarchical models applicable to
41 ocean circulation, atmospheric dispersion, and biological transport influenced by
42 oscillating currents.

43 **Keywords:** Inertial oscillations; Fluid parcel trajectories; Geophysical fluid dynamics;
44 Open-source programming languages; Idealized models

45 1 Introduction

46 The trajectory of neutrally buoyant fluid parcels in oscillating flows is a phenomenon
47 of profound significance within the realm of geophysical fluid dynamics (GFD), encom-
48 passing both oceanic and atmospheric contexts. Inertial oscillations, arising from the
49 intricate interplay between the Earth's rotation and fluid motions, exert a profound
50 influence on the behavior of these fluid parcels [1]. Accurately predicting the transport
51 and dispersion of tracers such as pollutants, nutrients, and biological organisms in the
52 oceans and atmosphere hinges on a comprehensive understanding of the trajectories
53 of non-buoyant particles subjected to such oscillating flows [2].

54 Geophysical fluids, including the vast oceans and the Earth's atmosphere, are
55 characterized by their immense spatial scales, intricate dynamics, and the pervasive
56 influence of rotational effects [3-5]. The Earth's rotation, manifesting through the
57 Coriolis force, introduces a unique set of challenges in precisely modeling fluid motions.
58 Inertial oscillations, also referred to as inertial waves or inertial currents, are a direct
59 manifestation of this rotational influence, causing fluid parcels to oscillate about their
60 mean trajectory due to the conservation of absolute angular momentum. This phe-
61 nomenon has far-reaching implications for the transport and mixing processes within
62 geophysical fluid systems.

63 While analytical solutions can provide valuable insights into the behavior of fluid
64 parcels under inertial oscillations, their applicability is often limited to highly simpli-
65 fied cases or requires restrictive assumptions, such as neglecting nonlinear effects or
66 assuming constant background flows. As a result, numerical simulations have emerged
67 as an indispensable tool for exploring the complex dynamics of these systems [6-8],
68 particularly in two-dimensional (2D) scenarios where the effects of vertical motions
69 are neglected. These idealized 2D models offer a crucial starting point for developing
70 intuition and understanding the fundamental physics governing fluid parcel trajec-
71 tories under the influence of inertial oscillations. Such parsimonious modeling efforts,

72 which strip away unnecessary complexities, are vital for gaining insights into the core
73 dynamics and informing more sophisticated hierarchical models.

74 In this study, we present a comprehensive numerical investigation of the 2D tra-
75 jectory of a non-buoyant fluid parcel subjected to inertial oscillations, a problem
76 of profound relevance in GFD. To ensure a thorough and robust analysis, we have
77 implemented the simulation using multiple open-source, code-based general program-
78 ming languages, including Fortran 95, Python, GNU Octave, R, and Julia. The choice
79 of these open-source languages not only promotes transparency and reproducibility
80 but also leverages the power of their extensive ecosystems and user communities,
81 facilitating collaborative development and knowledge sharing [9–11].

82 By running each implementation for 1,000 iterations, we aim to identify the most
83 efficient and reliable approach for simulating this phenomenon, providing valuable
84 insights into the selection of appropriate computational tools for similar numerical
85 simulations in the field of GFD. The use of general-purpose programming languages
86 offers flexibility, scalability, and the ability to integrate with a wide range of libraries
87 and tools, enabling seamless integration of visualization and analysis components.

88 Furthermore, we developed separate code modules specifically designed for visual-
89 izing the simulated trajectories using the powerful Matplotlib library in Python. These
90 visualization tools enable the generation of animated file, offering an intuitive and
91 dynamic representation of the particle’s motion over time. Such visualizations play a
92 crucial role in aiding the interpretation and communication of the results, facilitating
93 a deeper understanding of the underlying physics governing the trajectories of fluid
94 parcels under inertial oscillations.

95 The objectives of this paper are multifaceted. Firstly, we aim to provide a com-
96 prehensive and detailed description of the numerical methods employed in simulating
97 the 2D trajectory of a non-buoyant fluid parcel under inertial oscillations. Secondly,
98 we seek to evaluate the computational performance and accuracy of various open-
99 source programming languages in tackling this problem, thereby contributing to the
100 ongoing discourse on the selection of appropriate computational tools for numerical
101 simulations in GFD. Finally, we strive to contribute to the educational resources avail-
102 able for teaching and learning about idealized models in fluid dynamics, fostering a
103 deeper understanding of the fundamental principles governing fluid parcel trajectories
104 in rotating systems among students and researchers alike.

105 By addressing these objectives through a parsimonious modeling approach [12]
106 and leveraging the power of open-source, code-based general programming languages,
107 we aim to fill a crucial research gap by providing a comprehensive analysis of the
108 numerical simulation of this idealized problem. The insights gleaned from this study
109 will not only offer invaluable guidance on the selection of appropriate computational
110 tools for similar numerical simulations in GFD but also lay the foundation for devel-
111 oping more sophisticated hierarchical models [13]. The findings have the potential to
112 inform and advance a wide range of applications, from ocean circulation modeling [14]
113 to atmospheric dispersion studies [15], and from the tracking of marine debris to the
114 understanding of the transport of biological organisms influenced by oscillating cur-
115 rents [16]. Moreover, the idealized model and accompanying visualizations serve as

116 powerful educational resources, equipping students and researchers with the tools nec-
 117 essary to grasp the intricate interplay between fluid dynamics and rotational effects,
 118 ultimately fostering a deeper appreciation for the fundamental principles that govern
 119 the behavior of fluid parcels in rotating systems.

120 2 Methods

121 2.1 Mathematical Derivation

122 To define the motion of a fluid parcel influenced by inertial oscillations in two dimen-
 123 sions, the first step was to derive the Navier-Stokes equations specifically for a 2D
 124 scenario. Applying Newton’s second law to fluid dynamics, the Navier-Stokes equation
 125 accounts for the conservation of momentum. It integrates the effects of external forces,
 126 pressure gradients, and viscous forces within the fluid [17, 18]:

$$\rho \left(\frac{\partial \mathbf{u}}{\partial t} + \mathbf{u} \cdot \nabla \mathbf{u} \right) = -\nabla p + \mu \nabla^2 \mathbf{u} + \mathbf{f} \quad (1)$$

127 In this context, ρ defines the fluid density, and $\mathbf{u} \equiv (u, v)$ represents the fluid
 128 velocity vector, where u and v are the velocity components in the x and y directions,
 129 respectively. Furthermore, p denotes the pressure, μ signifies the dynamic viscosity,
 130 and \mathbf{f} refers to the body forces per unit volume. In the case of 2D flow, the Navier-
 131 Stokes equations can be separated into two components. One component represents
 132 the momentum equation in the x -direction and the other in the y -direction:

$$\begin{aligned} \rho \left(\frac{\partial u}{\partial t} + u \frac{\partial u}{\partial x} + v \frac{\partial u}{\partial y} \right) &= -\frac{\partial p}{\partial x} + \mu \left(\frac{\partial^2 u}{\partial x^2} + \frac{\partial^2 u}{\partial y^2} \right) + f_x \\ \rho \left(\frac{\partial v}{\partial t} + u \frac{\partial v}{\partial x} + v \frac{\partial v}{\partial y} \right) &= -\frac{\partial p}{\partial y} + \mu \left(\frac{\partial^2 v}{\partial x^2} + \frac{\partial^2 v}{\partial y^2} \right) + f_y \end{aligned} \quad (2)$$

133 To simplify our derivation of the Navier-Stokes equations for practical GFD appli-
 134 cations [3], several key assumptions were typically made. The fluid is treated as a
 135 Newtonian fluid, where the stress is linearly proportional to the strain rate. Under
 136 the continuum hypothesis, fluids are considered as continuous media. The assump-
 137 tion of incompressibility holds that the fluid density remains constant. Additionally,
 138 the fluid’s viscosity is considered constant, unaffected by changes in pressure, tem-
 139 perature, or velocity. The no-slip boundary condition is applied, meaning that fluid
 140 particles at solid boundaries exhibit no relative motion. Fluid properties are assumed
 141 isotropic, uniform in all directions. Generally, external forces other than body forces
 142 like gravity are ignored unless specifically stated.

143 To further refine our analysis of 2D inertial oscillation equations derived from the
 144 three-dimensional Navier-Stokes equation, we incorporated additional considerations
 145 about the flow dynamics and the assumptions under which we operated. We retained
 146 the assumption that the flow is predominantly horizontal ($w = 0$) with no vertical
 147 gradients ($\partial(\cdot)/\partial z$ terms are zero), which is suitable for scenarios where flow dynam-
 148 ics are limited to a thin layer, such as near the ocean surface or in the atmosphere
 149 away from significant topographical or frontal influences [e. g. 19–22]. In this context,
 150 we extended the geostrophic balance assumption by considering environments where

151 pressure gradient forces are negligible compared to the Coriolis and external forcing
 152 terms. This may occur in conditions with strong rotational effects or in areas where
 153 the pressure field is relatively uniform, minimizing the impact of pressure gradients
 154 on momentum balance.

155 Additionally, we considered external forcings that can influence the dynamics of
 156 the flow. We introduced forcings defined as:

$$\begin{aligned} f_x &= \frac{\partial u_f}{\partial t} \\ f_y &= \frac{\partial v_f}{\partial t} \end{aligned} \tag{3}$$

157 In this case, u_f represents a uniform external forcing in space, such as wind stress
 158 or other steady external influences. This assumption allows us to focus on the effect
 159 of external forcings on the fluid without the complications introduced by spatial
 160 variability.

161 In our simplified model, we ignored viscosity due to its minimal impact compared
 162 to inertial terms, and we continued to assume that the flow is irrotational, which sim-
 163 plifies the momentum equations. The Navier-Stokes equations then reduce primarily
 164 to expressions influenced by inertial effects and the Coriolis force, introduced through
 165 the Coriolis parameter f , twice the angular velocity of Earth's rotation [3]:

$$\begin{aligned} \frac{\partial u}{\partial t} &= -fv + f_x \\ \frac{\partial v}{\partial t} &= fu + f_y \end{aligned} \tag{4}$$

166 These equations govern the inertial oscillations in a rotating reference frame, sim-
 167 plified to highlight the oscillatory behavior of fluid parcels. We were particularly
 168 interested in predicting the pathway of a non-buoyant fluid parcel, which simplifies
 169 our assumptions further by neglecting buoyancy effects [3]. The pathway of these fluid
 170 parcels is then given by:

$$\begin{aligned} \frac{dx}{dt} &= U_0 + u \\ \frac{dy}{dt} &= V_0 + v \end{aligned} \tag{5}$$

171 In this context, U_0 and V_0 represent the ambient uniform flow, and u and v the
 172 velocity perturbations due to inertial oscillations. This model is highly simplified, and
 173 deriving this rigorously would involve linearizing the Navier-Stokes equations and pos-
 174 sibly introducing adjustments for external forcing terms and considering geostrophic
 175 balance if large-scale geophysical flows are being examined. This approach gives us
 176 a useful framework for understanding and predicting the movement of non-buoyant
 177 fluid parcels under specific geophysical conditions.

178 2.2 Numerical Experiments

179 The semi-implicit approach and the local rotation method are two numerical tech-
 180 niques used to predict the trajectory of non-buoyant fluid parcels in a rotating fluid

181 system, specifically addressing inertial oscillation problems. These methods offer dif-
 182 ferent perspectives and computational strategies to model the influence of the Coriolis
 183 force and other relevant factors.

184 Starting with the semi-implicit approach, we used the following numerical scheme
 185 to predict the trajectory of the fluid parcel as described in the equation 4:

$$\begin{aligned} u^{n+1} &= \frac{(1-\beta)u^n + \alpha v^n}{1+\beta} \\ v^{n+1} &= \frac{(1-\beta)v^n - \alpha u^n}{1+\beta} \end{aligned} \quad (6)$$

186 Here, u^n and v^n are the velocities at the current time step n , and u^{n+1} and v^{n+1}
 187 are the velocities at the next time step $n + 1$. The parameters α and β are defined as
 188 $\alpha = \Delta t f$ and $\beta = \frac{1}{4}\alpha$, respectively. This semi-implicit scheme efficiently integrates the
 189 inertial oscillation equations over time, providing accurate predictions of the fluid par-
 190 cel's velocity components (u, v) . To predict the x and y coordinates of a non-buoyant
 191 fluid parcel using this approach, we discretized the kinematic equation (equation 5)
 192 with finite differences:

$$\begin{aligned} \Delta x &= \frac{\alpha v^n}{1+\beta} \Delta t \\ \Delta y &= \frac{-\alpha u^n}{1+\beta} \Delta t \end{aligned} \quad (7)$$

193 Moving on to the local rotation method, we simulated the Coriolis force using a
 194 local rotation or velocity vector

$$\begin{aligned} u^{n+1} &= \cos(\theta)u^n + \sin(\theta)v^n \\ v^{n+1} &= \cos(\theta)v^n - \sin(\theta)u^n \end{aligned} \quad (8)$$

195 In this context, θ is determined based on the time step Δt and the Coriolis param-
 196 eter f , given by $\theta = 2 \sin^{-1}(\frac{1}{2}\Delta t f)$. For small $\Delta t|f|$, θ approximates $\Delta t f$. This method
 197 effectively captures the Coriolis effect by rotating the velocity components, aiding in
 198 predicting the trajectory of fluid parcels in a rotating system. By incorporating the
 199 finite difference approximation to the equation 5, we obtained:

$$\begin{aligned} \Delta x &= (\cos(\theta) - 1) u^n \Delta t + \sin(\theta) v^n \Delta t \\ \Delta y &= \cos(\theta) v^n \Delta t - (\sin(\theta) + 1) u^n \Delta t \end{aligned} \quad (9)$$

200 By discretizing these equations and incorporating the velocity updates from semi-
 201 implicit and/or local rotation schemes, we were able to iteratively predict the x and y
 202 coordinates of fluid parcels over time. In that study, we aimed to use these numerical
 203 schemes to predict the trajectory of a non-buoyant fluid parcel floating with ambient
 204 uniform flow (U_0, V_0) , which is sometimes influenced by abrupt wind events. In that
 205 simulation, we modeled the ambient flow as a uniform northeastward flow with values
 206 of $U_0 = 5$ cm/s and $V_0 = 5$ cm/s. The total simulation time is 6 days with $\Delta t = 4320$
 207 seconds, approximately 1.2 days. There were three abrupt events that changed the

208 relative flow speed and direction $(\Delta u_f, \Delta v_f)$. These changes were explained in Table
209 1 as follows.

Table 1: Velocity disturbance parameters.

| time (days) | Δu_f (cm / s) | Δv_f (cm / s) |
|-------------|-----------------------|-----------------------|
| 1 | 10 | 0 |
| 2 | 10 | 0 |
| 4 | 0 | 10 |

210 To tackle this issue, we explored various numerical schemes within several open-
211 source computing environments highly regarded in earth science and specifically GFD.
212 Initially, we applied these schemes using Fortran, a language with a long history in
213 solving such problems [e. g. 23–26]. Fortran remains widely used today, especially in
214 general circulation models (GCMs) [27]. For instance, the 1995 version of Fortran has
215 been pivotal in many classic problem-solving scenarios within this domain [28, 29].

216 Another avenue we pursued was implementing the solutions in Python, leveraging
217 the NumPy library [30]. Python has emerged as a dominant force in programming
218 due to its versatility and extensive libraries like NumPy, which are invaluable for
219 numerical simulations and statistical computations in earth sciences [e. g. 31–35].
220 Its modern features make it a go-to choice for researchers and practitioners alike.
221 Moreover, we explored GNU Octave, an open-source platform akin to MATLAB[®] but
222 freely available. Its syntax, resembling MATLAB[®]'s, appeals to those familiar with
223 MATLAB[®] but seeking a cost-effective solution. This makes it a viable option for
224 GFD modelers and researchers interested in numerical computations [e. g. 36–38].

225 Additionally, we delved into Julia, a computing environment gaining traction
226 among GFD modelers. Julia's ability to match Fortran's speed while maintaining
227 Python's ease of understanding has attracted attention. Many are considering transi-
228 tioning from Fortran to Julia for ocean models due to this combination of speed and
229 user-friendliness [e. g. 37, 39–43]. Lastly, we conducted numerical calculations in R, a
230 popular choice within the atmospheric and oceanic sciences communities [e. g. 44–47].
231 R's strengths in data analysis and visualization make it a valuable tool for researchers
232 working with numerical data in these fields.

233 Following the numerical calculations in various computing environments, we pre-
234 served the resulting simulation data in a structured format as a text file. This data
235 storage method ensures that the data remains accessible and can be easily manipu-
236 lated for further analysis or visualization. For visualization purposes, we turned to the
237 Matplotlib library [48] within the Python computing environment. Matplotlib offers
238 a robust suite of tools for creating static plots and animations, making it a preferred
239 choice among researchers and practitioners in data visualization. The process involved
240 writing a separate code specifically for plotting and animating the simulation results.

241 Once the plotting and animation code was executed, we generated two distinct out-
242 puts: a static plot saved in Portable Network Graphics (**.png**) format and an animation
243 saved in Graphics Interchange Format (**.gif**). These formats are widely supported

244 and compatible with various platforms, ensuring the accessibility and usability of the
 245 visualized data across different systems and applications. The static plot provides a
 246 snapshot of the simulation results, while the animation offers a dynamic representation,
 247 capturing temporal variations and trends within the data.

248 2.3 Statistical Analysis

249 Our next steps was to employ a Python code to rigorously evaluate and compare the
 250 execution times of code across diverse programming languages, aiding in informed
 251 language selection for scientific tasks. We began by compiling a Fortran code using
 252 the gfortran compiler, recording the compilation time for insights into overhead. Once
 253 compiled, the Python code executed each numerical solver for 1,000 times, ensuring
 254 robust statistical sampling. Crucial metrics like execution time, return codes, standard
 255 output, and errors were captured using the Subprocess library. Code was executed
 256 based on file extensions: Fortran via the compiled executable, and others (Python,
 257 Julia, MATLAB, and R) using their respective interpreters or runtimes. Data for
 258 each run included code details, execution time, return codes for error handling, and
 259 output/error messages. The resulting dataset was structured into a Pandas DataFrame
 260 [49] and exported to comma-separated values (.csv) for analysis.

261 For statistical comparison, we applied the Kruskal-Wallis (KW) test , a non-
 262 parametric method suitable for comparing multiple independent groups [50]. The
 263 Kruskal-Wallis test evaluates the null hypothesis that the medians of all groups
 264 are equal, indicating no significant difference in performance among programming
 265 languages. This test produces a test statistic H along with a p-value:

$$H = \frac{12}{N(N+1)} \sum_{j=1}^k \frac{R_j^2}{n_j} - 3(N+1) \quad (10)$$

266 In this case, N is the total number of observations, k is the number of groups, n_j
 267 is the number of observations in the j th group, and R_j is the sum of ranks for the j th
 268 group. The degrees of freedom for the Kruskal-Wallis test is $df = k - 1$.

269 If the p-value from the KW test is below a pre-defined significance level $\alpha = 0.05$,
 270 we proceeded with Dunn’s post-hoc test. Dunn’s test is used for pairwise comparisons
 271 between groups to identify which groups exhibit statistically significant differences in
 272 performance [51].

273 Dunn’s test statistic for pairwise comparisons between groups i and j is given by:

$$Z_{ij} = \frac{|R_i - R_j| - (N(N+1))/12}{\sqrt{N(N+1)(N+2)/12}} \quad (11)$$

274 The critical value for Dunn’s test is obtained using the Bonferroni adjustment,
 275 where the significance level α is divided by the number of pairwise comparisons m
 276 to control for multiple testing:

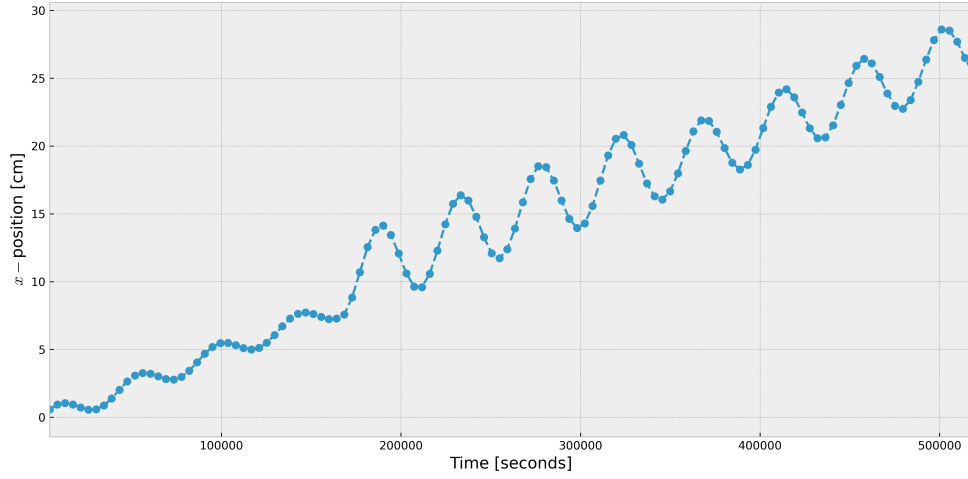
$$\alpha_{\text{adjusted}} = \frac{\alpha}{m} \quad (12)$$

277 Pairwise comparisons with $|Z_{ij}|$ exceeding the adjusted critical value indicate
 278 statistically significant differences between the corresponding groups. We performed

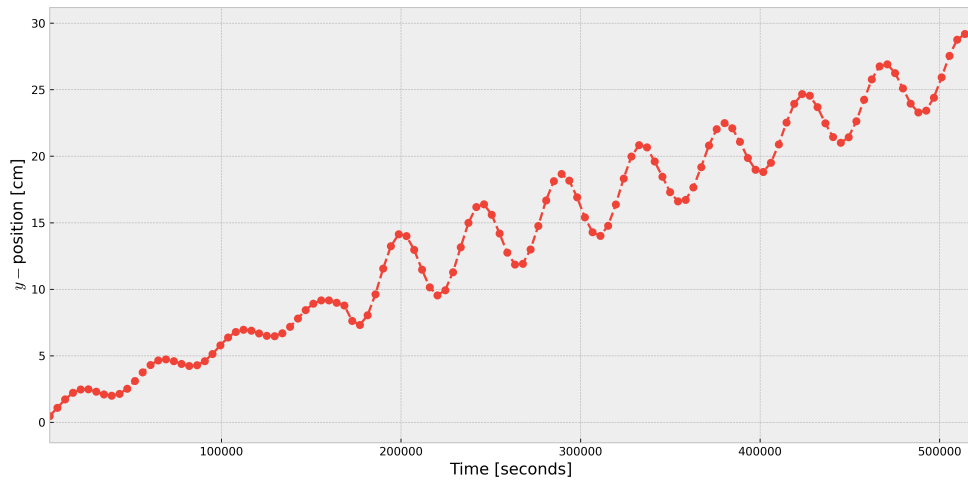
279 these calculations automatically using the statistics module in the SciPy [52] and
280 the scikit-posthoc [53] libraries in the Python computing environment. This rigorous
281 statistical approach ensured reliable insights into the computational performance of
282 multiple computing environments for simulating a 2D fluid parcel trajectory over 1,000
283 iterations.

284 **3 Results and Discussion**

285 Simulations modeled the trajectory of a non-buoyant fluid parcel under the combined
286 influence of inertial oscillations induced by the Earth's rotation, a uniform ambient
287 northeasterly flow over six days, and abrupt disturbance events on days one, two,
288 and four. Figures 1a and 1b depict oscillatory trajectories plotted against time. Both
289 exhibit increasing amplitude due to Coriolis effects, but with slight path deviations
290 attributable to numerical precision.



(a)



(b)

Fig. 1: Temporal evolution of a non-buoyant fluid parcel undergoing inertial oscillation and abrupt forcing events in (a) x and (b) y directions.

291 Figure 2 reveals a spiraling cyclical trajectory forming expanding loops - the
 292 expected inertial oscillation pattern. However, distinct perturbations are evident, likely
 293 caused by the simulated disturbance events capable of amplifying or damping the
 294 oscillations, with profound impacts on parcel transport and dispersion. The increasing
 295 oscillation amplitudes accurately capture the conservation of absolute angular momen-
 296 tum as the Coriolis force deflects the parcel from its mean path. Superimposed ambient

297 flow adds an advective component, further complexifying the trajectory. Observed tra-
298 jectory patterns validate the numerical models' ability to represent the fundamental
299 rotational dynamics governing fluid motion in this idealized scenario. While implemen-
300 tation differences were minor here, they highlight the importance of numerical accuracy
301 and algorithm design for faithfully representing intricate fluid behavior, which could
302 be amplified under more complex conditions. Because this paper is static, we were not
303 displaying the trajectory animation from Fig. 2. If readers are interested in obtaining
304 it, they can visit our GitHub page as mentioned in the Acknowledgments section.

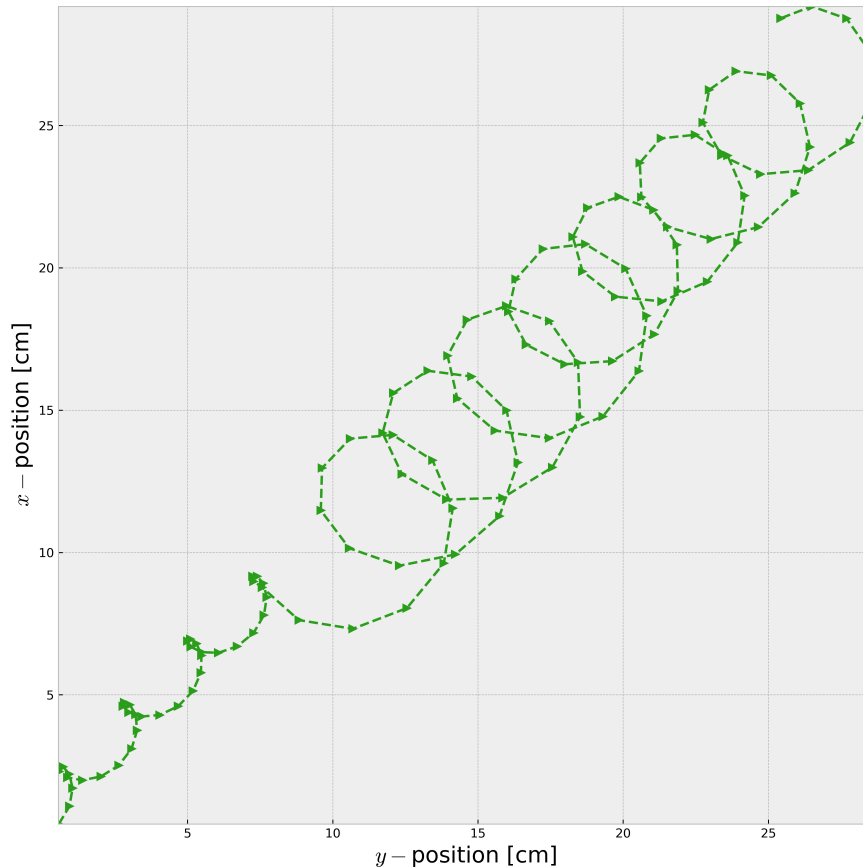


Fig. 2: The trajectory of a fluid element propelled within an ambient flow and under-
going inertial oscillation.

305 Figure 3 examines the execution times of various computing environments for sim-
306 ulating the trajectory of a fluid parcel under inertial oscillations in a two-dimensional
307 geophysical fluid system. 1,000 simulations were run in each environment: Fortran,
308 Python, Julia, GNU Octave, and R. The execution time is measured in seconds.

309 The results reveal Fortran as the clear leader in terms of both speed and con-
310 sistency. The boxplots visually demonstrate this by clustering the majority of data
311 points around the median for Fortran. Statistical data reinforces this observation. The
312 mean execution time (0.01 seconds) for Fortran closely aligns with the median (0.01
313 seconds), indicating a symmetrical distribution with minimal outliers impacting the
314 mean. Furthermore, the exceptionally low standard deviation of 0.001 seconds for For-
315 tran underscores the remarkable consistency achieved in execution times within this
316 environment.

317 In contrast, Python, R, Julia, and GNU Octave exhibit greater variability in execu-
318 tion times, as evidenced by the larger interquartile ranges (IQRs) and the presence of
319 outliers. Among these environments, Python delivers a median execution time of 0.47
320 seconds, which is faster than both R (1.01 seconds) and GNU Octave (0.52 seconds).
321 Additionally, Python boasts a relatively small IQR of 0.064 seconds. However, Julia
322 lags behind considerably with a median execution time of 3.8 seconds and a larger
323 IQR of 1.14 seconds. This signifies that half of the simulations in Julia took between
324 3.12 and 4.26 seconds to complete. The standard deviations further substantiate this
325 variability. Julia exhibits the largest standard deviation (0.593 seconds) compared to
326 Python (0.046 seconds) and GNU Octave (0.090 seconds). The presence of outliers in
327 Julia (one at 6.86 seconds) and Octave (one at 1.69 seconds) reinforces this observation.

328 The choice of the most suitable environment may depend on other factors beyond
329 just execution time. These factors include ease of use and coding expertise required
330 for each language, availability of libraries or functionalities specific to the scientific
331 domain, and memory usage and scalability for larger datasets. It would be beneficial to
332 investigate the reasons behind the slower and more variable execution times observed
333 in Julia, Python, and GNU Octave. One possibility is that the code implementations
334 in these environments might be less optimized compared to Fortran. Further analysis
335 could involve code profiling to identify performance bottlenecks in Julia, Python, and
336 GNU Octave.

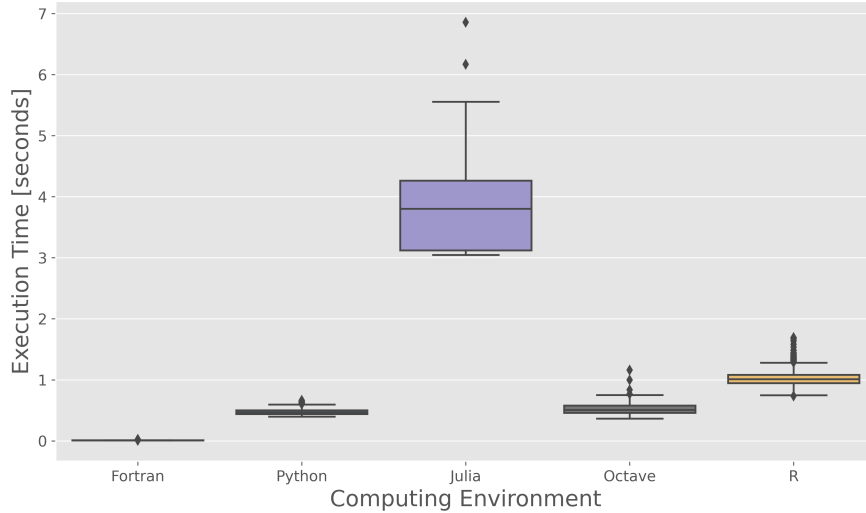


Fig. 3: Box plots comparing the execution times of simulating the 2D trajectory of a non-buoyant fluid parcel under inertial oscillations using different open-source programming languages (Fortran, Python, Julia, GNU Octave, and R) over 1,000 iterations.

337 Statistical analysis was employed to rigorously evaluate the execution time varia-
 338 tions across five computing environments: Fortran, Julia, GNU Octave, Python, and
 339 R. The KW test, a non-parametric method for comparing medians across multiple
 340 groups, was conducted. The test yielded a statistically significant result (p-value =
 341 0.000, test statistic = 4577.973), rejecting the null hypothesis that the medians of all
 342 environments were equal. This confirms the initial observations from the boxplots,
 343 suggesting at least one environment exhibits a median execution time demonstrably
 344 different from the others.

345 To identify environments with statistically distinct medians, Dunn’s post-hoc test
 346 with Bonferroni correction was utilized. This correction accounts for multiple com-
 347 parisons and minimizes the likelihood of false positives. The results corroborated
 348 Fortran’s exceptional performance. Execution times in Fortran were statistically dif-
 349 ferent from all other environments (Julia, Octave, Python, and R) at a significance
 350 level of $\alpha = 0.05$ (all p-values were 0.000). This translates to a significantly faster
 351 median execution time for Fortran compared to the other environments. Furthermore,
 352 pairwise comparisons among Julia, GNU Octave, Python, and R revealed statistically
 353 significant differences in their median execution times as well (all p-values were 0.000)
 354 (Fig. 4). However, the specific order of their performance remains undetermined from
 355 the this test.

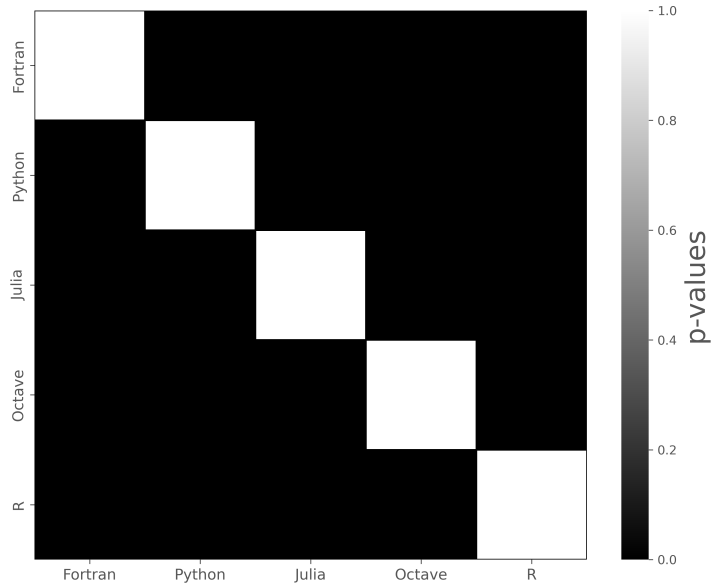


Fig. 4: Heatmap of p-values from Dunn’s test (Bonferroni adjusted) comparing the computational performance of programming languages (Fortran, Python, Julia, GNU Octave, and R) in simulating a 2D fluid parcel trajectory over 1,000 iterations. Black shades indicate statistically significant performance differences.

356 This statistical analysis strongly supports the initial observations. Fortran emerged
 357 as the clear leader in terms of execution speed, boasting a median time demonstrably
 358 faster than all other environments. Julia, GNU Octave, Python, and R exhibited
 359 greater variability in execution times and statistically significant differences in their
 360 medians compared to each other. Further investigation, potentially focusing on code
 361 optimization within these environments, could be insightful in elucidating the reasons
 362 behind these variations.

363 4 Conclusion

364 The numerical simulation of the trajectory of a non-buoyant fluid parcel under inertial
 365 oscillation in a two-dimensional geophysical fluid system provides valuable insights
 366 into the fundamental physics governing fluid parcel transport and dispersion. By lever-
 367 aging open-source programming languages, this study not only contributes to the
 368 reproducibility and transparency of scientific research but also facilitates collaborative
 369 knowledge sharing within the GFD communities.

370 The evaluation of computational performance across multiple programming envi-
371 ronments, including Fortran, Python, Julia, GNU Octave, and R, revealed Fortran
372 as the most efficient choice for simulating this idealized scenario. Statistical anal-
373 ysis confirmed that Fortran exhibited significantly faster execution times compared
374 to the other environments, highlighting its suitability for computationally intensive
375 numerical simulations in GFD. However, the selection of an appropriate program-
376 ming language should also consider factors such as coding expertise, availability of
377 specialized libraries, and scalability requirements.

378 Ultimately, this study serves as a foundation for developing more sophisticated
379 hierarchical models that capture the intricate dynamics of fluid parcel trajectories in
380 rotating systems. The insights gained from this idealized model have the potential to
381 inform a wide range of applications.

382 **Acknowledgments.** We extend our sincere gratitude to Andrew J. Ridgwell, Gay-
383 atri Mishra, and Sandra K. Turner for their invaluable discussions on geophysical
384 fluid dynamics within oceanic realms, and to Faiz R. Fajary for insightful conversa-
385 tions regarding atmospheric dynamics. Their collective expertise greatly enriched our
386 understanding and contributed significantly to this work. We are also grateful for the
387 generous support from the Dean’s Distinguished Fellowship at the University of Cal-
388 ifornia, Riverside (UCR) in 2023 and the ITB Research, Community Services, and
389 Innovation Program (PPMI-ITB) in 2024, which made this research possible. The
390 code and complete runtime dataset associated with this paper are accessible through
391 our GitHub repository: <https://github.com/sandyherho/inerOsci>.

392 References

- 393 [1] Hasselmann, K.: Wave-driven inertial oscillations. *Geophys. Astrophys. Fluid*
394 *Dyn.* **1**(3-4), 463–502 (1970) <https://doi.org/10.1080/03091927009365783>
- 395 [2] Voisin, B.: Buoyancy oscillations. *J. Fluid Mech.* **984**, 29 (2024) [https://doi.org/](https://doi.org/10.1017/jfm.2024.179)
396 [10.1017/jfm.2024.179](https://doi.org/10.1017/jfm.2024.179)
- 397 [3] Cushman-Roisin, B., Beckers, J.-M.: *Introduction to Geophysical Fluid Dynam-*
398 *ics: Physical and Numerical Aspects.* Academic Press, Oxford (2011)
- 399 [4] Pedlosky, J.: *Geophysical Fluid Dynamics.* Springer, Berlin (2013)
- 400 [5] Vallis, G.K.: Geophysical fluid dynamics: whence, whither and why? *Proc. Math.*
401 *Phys. Eng. Sci.* **472**(2192), 20160140 (2016) [https://doi.org/10.1098/rspa.2016.](https://doi.org/10.1098/rspa.2016.0140)
402 [0140](https://doi.org/10.1098/rspa.2016.0140)
- 403 [6] Denton, J.D., Dawes, W.N.: Computational fluid dynamics for turbomachinery
404 design. *Proc. Inst. Mech. Eng., Part C* **213**(2), 107–124 (1998) [https://doi.org/](https://doi.org/10.1243/0954406991522211)
405 [10.1243/0954406991522211](https://doi.org/10.1243/0954406991522211)
- 406 [7] Malki, R., Williams, A.J., Croft, T.N., Togneri, M., Masters, I.: A coupled blade
407 element momentum–Computational fluid dynamics model for evaluating tidal

- 408 stream turbine performance. *Appl. Math. Model.* **37**(5), 3006–3020 (2013) <https://doi.org/10.1016/j.apm.2012.07.025>
409
- 410 [8] Windt, C., Davidson, J., Ringwood, J.V.: High-fidelity numerical modelling of
411 ocean wave energy systems: A review of computational fluid dynamics-based
412 numerical wave tanks. *Renewable and Sustainable Energy Reviews* **93**, 610–630
413 (2018) <https://doi.org/10.1016/j.rser.2018.05.020>
- 414 [9] Bhatt, A., Valentic, T., Reimer, A., Lamarche, L., Reyes, P., Cosgrove, R.: Repro-
415 ducible Software Environment: a tool enabling computational reproducibility in
416 geospace sciences and facilitating collaboration. *J. Space Weather Space Clim.*
417 **10**, 12 (2020) <https://doi.org/10.1051/swsc/2020011>
- 418 [10] Talirz, L., Kumbhar, S., Passaro, E., Yakutovich, A.V., Granata, V., Gargiulo,
419 F., Borelli, M., Uhrin, M., Huber, S.P., Zoupanos, S., Adorf, C.S., Andersen,
420 C.W., Schütt, O., Pignedoli, C.A., Passerone, D., VandeVondele, J., Schulthess,
421 T.C., Smit, B., Pizzi, G., Marzari, N.: Materials Cloud, a platform for open
422 computational science. *Sci. Data* **7**(1), 299 (2020) <https://doi.org/10.1038/s41597-020-00637-5>
423
- 424 [11] Beg, M., Taka, J., Kluyver, T., Konovalov, A., Ragan-Kelley, M., Thiéry, N.M.,
425 Fangohr, H.: Using Jupyter for reproducible scientific workflows. *Comput. Sci.*
426 *Eng.* **23**(2), 36–46 (2021) <https://doi.org/10.1109/MCSE.2021.3052101>
- 427 [12] Lazar, N.: Ockham’s razor. *Wiley Interdiscip. Rev. Comput. Stat.* **2**(2), 243–246
428 (2010) <https://doi.org/10.1002/wics.75>
- 429 [13] Jeevanjee, N., Hassanzadeh, P., Hill, S., Sheshadri, A.: A perspective on climate
430 model hierarchies. *J. Adv. Model. Earth Syst.* **9**(4), 1760–1771 (2017) <https://doi.org/10.1002/2017MS001038>
431
- 432 [14] Song, D., Gao, G., Xia, Y., Ren, Z., Liu, J., Bao, X., Yin, B.: Near-inertial
433 oscillations in seasonal highly stratified shallow water. *Estuar. Coast. Shelf Sci.*
434 **258**, 107445 (2021) <https://doi.org/10.1016/j.ecss.2021.107445>
- 435 [15] Mirza, A.K., Dacre, H.F., Lo, C.H.B.: A case study analysis of the impact of
436 a new free tropospheric turbulence scheme on the dispersion of an atmospheric
437 tracer. *Q. J. R. Meteorol. Soc.* (2024) <https://doi.org/10.1002/qj.4681>
- 438 [16] Beron-Vera, F.J.: Nonlinear dynamics of inertial particles in the ocean: From
439 drifters and floats to marine debris and *Sargassum*. *Nonlinear Dynamics* **103**(1),
440 1–26 (2021) <https://doi.org/10.1007/s11071-020-06053-z>
- 441 [17] Ershkov, S.V., Prosviryakov, E.Y., Burmasheva, N.V., Christianto, V.: Towards
442 understanding the algorithms for solving the Navier–Stokes equations. *Fluid Dyn.*
443 *Res.* **53**(4), 044501 (2021) <https://doi.org/10.1088/1873-7005/ac10f0>

- 444 [18] Garvin, J.W.: A Student's Guide to the Navier-Stokes Equations. Cambridge
445 University Press, Cambridge (2023)
- 446 [19] Li, R., Chen, C., Dong, W., Beardsley, R.C., Wu, Z., Gong, W., Liu, Y., Liu,
447 T., Xu, D.: Slope-intensified storm-induced near-inertial oscillations in the South
448 China sea. *J. Geophys. Res. Oceans* **126**(3), 2020–016713 (2021) [https://doi.org/
449 10.1029/2020JC016713](https://doi.org/10.1029/2020JC016713)
- 450 [20] Hibiya, T.: A new parameterization of turbulent mixing enhanced over rough
451 seafloor topography. *Geophys. Res. Lett.* **49**(2), 2021–096067 (2022) [https://doi.
452 org/10.1029/2021GL096067](https://doi.org/10.1029/2021GL096067)
- 453 [21] Luo, X., Huang, X., Fei, J., Wang, J., Li, C., Cheng, X.: Role of Topography in
454 Triggering Elevated Thunderstorms Associated With Winter Cold Fronts Over
455 the Eastern Yunnan-Guizhou Plateau. *J. Geophys. Res. Atmos.* **128**(8), 2023–
456 038640 (2023) <https://doi.org/10.1029/2023JD038640>
- 457 [22] Zhu, Y., Liang, X.: Near-inertial oscillations in the deep Gulf of Mexico. *Deep-
458 Sea Res. II: Top. Stud. Oceanogr.* **210**, 105310 (2023) [https://doi.org/10.1016/j.
459 dsr2.2023.105310](https://doi.org/10.1016/j.dsr2.2023.105310)
- 460 [23] Price, E., Mielikainen, J., Huang, M., Huang, B., Huang, H.-L.A., Lee, T.: GPU-
461 accelerated longwave radiation scheme of the rapid radiative transfer model for
462 general circulation models (RRTMG). *IEEE J. Sel. Top. Appl. Earth Obs. Remote
463 Sens.* **7**(8), 3660–3667 (2014) <https://doi.org/10.1109/JSTARS.2014.2315771>
- 464 [24] Norman, M., Larkin, J., Vose, A., Evans, K.: A case study of CUDA FORTRAN
465 and OpenACC for an atmospheric climate kernel. *J. Comput. Sci.* **9**, 1–6 (2015)
466 <https://doi.org/10.1016/j.jocs.2015.04.022>
- 467 [25] Ott, J., Pritchard, M., Best, N., Linstead, E., Curcic, M., Baldi, P.: A Fortran-
468 Keras deep learning bridge for scientific computing. *Sci. Program.* **2020**, 1–13
469 (2020) <https://doi.org/10.1155/2020/8888811>
- 470 [26] Perkins, W.A., Brenowitz, N.D., Bretherton, C.S., Nugent, J.M.: Emulation of
471 cloud microphysics in a climate model. *J. Adv. Model. Earth Syst.* **16**(4), 2023–
472 003851 (2024) <https://doi.org/10.1029/2023MS003851>
- 473 [27] Held, I.M., Suarez, M.J.: A Proposal for the Intercomparison of the Dynamical
474 Cores of Atmospheric General Circulation Models. *Bull. Am. Meteorol. Soc.*
475 **75**(10), 1825–1830 (1994)
- 476 [28] Kämpf, J.: *Ocean Modelling for Beginners: Using Open-source Software*. Springer,
477 Berlin (2009)
- 478 [29] Kämpf, J.: *Advanced Ocean Modelling: Using Open-Source Software*. Springer,
479 Berlin (2010)

- 480 [30] Van Der Walt, S., Colbert, S.C., Varoquaux, G.: The NumPy array: a structure
481 for efficient numerical computation. *Comput. Sci. Eng.* **13**(2), 22–30 (2011) <https://doi.org/10.1109/MCSE.2011.37>
482
- 483 [31] Herho, S.H.S., Irawan, D.E.: PY-METEO-NUM: Dockerized Python Notebook
484 Environment for Portable Data Analysis Workflows in Indonesian Atmospheric
485 Science Communities. *Int. J. Data Sci.* **2**(1), 38–46 (2021) <https://doi.org/10.18517/ijods.2.1.38-46.2021>
486
- 487 [32] Herho, S.H.S.: A Univariate Extreme Value Analysis and Change Point Detection
488 of Monthly Discharge in Kali Kupang, Central Java, Indonesia. *JOIV : Int. J.*
489 *Inform. Visualization* **6**(4), 862–868 (2022) <https://doi.org/10.30630/joiv.6.4.953>
- 490 [33] Qian, Y.-K.: xinvert: A Python package for inversion problems in geophysical fluid
491 dynamics. *J. Open Source Softw.* **8**(89), 5510 (2023) <https://doi.org/10.21105/joss.05510>
492
- 493 [34] Yu, J., Mukerji, T., Avseth, P.: rockphypy: An extensive Python library for rock
494 physics modeling. *SoftwareX* **24**, 101567 (2023) <https://doi.org/10.1016/j.softx.2023.101567>
495
- 496 [35] Suwarman, R., Herho, S., Belgaman, H., Ichiyanagi, K., Uesugi, T., Irawan, D.,
497 Yosa, I., Utami, A., Prayogo, S., Aldrian, E.: imc-precip-iso: open monthly stable
498 isotope data of precipitation over the Indonesian Maritime Continent. *J. of Data,*
499 *Inf. and Manag.*, 1–12 (2024) <https://doi.org/10.1007/s42488-024-00116-1>
- 500 [36] Jaffrés, J.B.D.: GHCN-Daily: a treasure trove of climate data awaiting discovery.
501 *Comput. Geosci.* **122**, 35–44 (2019) <https://doi.org/10.1016/j.cageo.2018.07.003>
- 502 [37] Sulpis, O., Humphreys, M.P., Wilhelmus, M.M., Carroll, D., Berelson, W.M.,
503 Menemenlis, D., Middelburg, J.J., Adkins, J.F.: RADIV1: a non-steady-state
504 early diagenetic model for ocean sediments in Julia and MATLAB/GNU
505 Octave. *Geosci. Model Dev.* **15**(5), 2105–2131 (2022) <https://doi.org/10.5194/gmd-15-2105-2022>
506
- 507 [38] Jaffrés, J.B.D., Gray, J.L.: Chasing rainfall: estimating event precipitation along
508 tracks of tropical cyclones via reanalysis data and in-situ gauges. *Environ. Model.*
509 *Softw.* **167**, 105773 (2023) <https://doi.org/10.1016/j.envsoft.2023.105773>
- 510 [39] Perkel, J.M.: Julia: come for the syntax, stay for the speed. *Nature* **572**(7767),
511 141–142 (2019) <https://doi.org/10.1038/d41586-019-02310-3>
- 512 [40] Ramadhan, A., Wagner, G., Hill, C., Campin, J.-M., Churavy, V., Besard, T.,
513 Souza, A., Edelman, A., Ferrari, R., Marshall, J.: Oceananigans.jl: Fast and
514 friendly geophysical fluid dynamics on GPUs. *J. Open Source Softw.* **5**(53) (2020)
515 <https://doi.org/10.21105/joss.02018>

- 516 [41] Constantinou, N., Wagner, G., Siegelman, L., Pearson, B., Palóczy, A.: GeophysicalFlows.jl: Solvers for geophysical fluid dynamics problems in periodic domains
517 on CPUs GPUs. *J. Open Source Softw.* **6**(60) (2021) [https://doi.org/10.21105/](https://doi.org/10.21105/joss.03053)
518 [joss.03053](https://doi.org/10.21105/joss.03053)
519
- 520 [42] Partee, S., Ellis, M., Rigazzi, A., Shao, A.E., Bachman, S., Marques, G., Robbins,
521 B.: Using machine learning at scale in numerical simulations with SmartSim:
522 An application to ocean climate modeling. *J. Comput. Sci.* **62**, 101707 (2022)
523 <https://doi.org/10.1016/j.jocs.2022.101707>
- 524 [43] Bishnu, S., Strauss, R.R., Petersen, M.R.: Comparing the Performance of Julia
525 on CPUs versus GPUs and Julia-MPI versus Fortran-MPI: a case study with
526 MPAS-Ocean (Version 7.1). *Geosci. Model Dev.* **16**(19), 5539–5559 (2023) <https://doi.org/10.5194/gmd-16-5539-2023>
527
- 528 [44] Czernecki, B., Głogowski, A., Nowosad, J.: Climate: An R package to access free
529 in-situ meteorological and hydrological datasets for environmental assessment.
530 *Sustainability* **12**(1), 394 (2020) <https://doi.org/10.3390/su12010394>
- 531 [45] Herho, S.H.S., Brahmana, F., Herho, K.E.P., Irawan, D.E.: Does ENSO sig-
532 nificantly affect rice production in Indonesia? A preliminary study using com-
533 putational time-series approach. *Int. J. Data Sci.* **2**(2), 69–76 (2021) <https://doi.org/10.18517/ijods.2.2.69-76.2021>
534
- 535 [46] McKay, N.P., Emile-Geay, J., Khider, D.: GeoChronR—an R package to model,
536 analyze and visualize age-uncertain paleoscientific data. *Geochronology* **2020**,
537 1–33 (2020) <https://doi.org/10.5194/gchron-3-149-2021>
- 538 [47] Ashkezari, M.D., Hagen, N.R., Denholtz, M., Neang, A., Burns, T.C., Morales,
539 R.L., Lee, C.P., Hill, C.N., Armbrust, E.V.: Simons collaborative marine atlas
540 project (Simons CMAP): an open-source portal to share, visualize, and analyze
541 ocean data. *Limnol. Oceanogr. Methods* **19**(7), 488–496 (2021) <https://doi.org/10.1002/lom3.10439>
542
- 543 [48] Hunter, J.D.: Matplotlib: A 2D graphics environment. *Comput. Sci. Eng.* **9**(03),
544 90–95 (2007) <https://doi.org/10.1109/MCSE.2007.55>
- 545 [49] McKinney, W.: pandas: a foundational Python library for data analysis and
546 statistics. *Python for High Performance and Scientific Computing* **14**(9), 1–9
547 (2011)
- 548 [50] Ostertagova, E., Ostertag, O., Kováč, J.: Methodology and application of the
549 Kruskal-Wallis test. *Appl. Mech.* **611**, 115–120 (2014) [https://doi.org/10.4028/](https://doi.org/10.4028/www.scientific.net/AMM.611.115)
550 [www.scientific.net/AMM.611.115](https://doi.org/10.4028/www.scientific.net/AMM.611.115)
- 551 [51] Ruxton, G.D., Beauchamp, G.: Time for some a priori thinking about post
552 hoc testing. *Behav. Ecol.* **19**(3), 690–693 (2008) <https://doi.org/10.1093/beheco/>

- 554 [52] Virtanen, P., Gommers, R., Oliphant, T.E., Haberland, M., Reddy, T., Cournapeau, D., Burovski, E., Peterson, P., Weckesser, W., Bright, J., van der Walt, S.J., Brett, M., Wilson, J., Millman, K.J., Mayorov, N., Nelson, A.R.J., Jones, E., Kern, R., Larson, E., Carey, C.J., Polat, İ., Feng, Y., Moore, E.W., VanderPlas, J., Laxalde, D., Perktold, J., Cimrman, R., Henriksen, I., Quintero, E.A., Harris, C.R., Archibald, A.M., Ribeiro, A.H., Pedregosa, F., van Mulbregt, P., SciPy 1.0 Contributors: SciPy 1.0: Fundamental Algorithms for Scientific Computing in Python. *Nat. Methods* **17**, 261–272 (2020) <https://doi.org/10.1038/s41592-019-0686-2>
- 563 [53] Terpilowski, M.A.: scikit-posthocs: Pairwise multiple comparison tests in Python. *J. Open Source Softw.* **4**(36), 1169 (2019) <https://doi.org/10.21105/joss.01169>
- 564